S**upplemental figure legends**

Fig. S1. Schematic representation of FP assay and AFM analysis of preformed Aβ42 seeds. (a) Schematic representation of FP assay. A mixture of unlabeled Aβ42 monomers and 5-Carboxyfluorescein-labelled Aβ42 peptide tracer molecules (^{FAM}Aβ42) was incubated at 37 °C in a microtiter plate. This leads to the formation of fluorescently labelled fibrillar ^{FAM}Aβ42/Aβ42 co-aggregates that grow larger in their size with time. By quantification of fluorescent polarization (FP) the growth of ^{FAM}Aβ42/Aβ42 co-aggregates can be monitored in a time-dependent manner. For FAM molecules attached to small, rapidly rotating peptides (e.g., monomers) the initially photoselected orientational distribution becomes randomized prior to emission, resulting in low FP. Conversely, incorporation of FAM-conjugated tracer peptides into large, slowly rotating ^{FAM}Aβ42/Aβ42 co-aggregates results in high FP. Thus, FP measurement provides a direct readout for the time-dependent formation of large, fibrillar ^{FAM}Aβ42/Aβ42 co-aggregates in cell-free assays. **(b)** AFM analysis of preformed Aβ42 seeds. Atomic force microscopy (AFM) analysis of preformed β-sheet-rich Aβ42 fibrillar assemblies utilized as seeds to stimulate ^{FAM}Aβ42/Aβ42 co-aggregation in FP assays.

Fig. S2. Seed-mediated Aβ42 aggregation. **(a)** Analysis of Aβ aggregates enriched by immunoprecipitation from brain extracts of transgenic APPPS1 mice by SDS-PAGE and immunoblotting using the 6E10 anti-amyloid antibody. **(b)** Analysis of 6E10-immunoprecipitated material from APPPS1 mouse brain extracts by Coomasie blue R staining of SDS gels **(C)** BN-PAGE and immunoblot analysis of seeded SCL-treated (10 µM) and untreated ^{FAM}Aβ42/Aβ42 co-aggregation (0.1/ 10 µM) reactions. Reactions were seeded with preformed β-sheet-rich fibrillar Aβ42 aggregates (100 nM, monomer equivalent). **(d)** AFM examination of seeded (100 nM seeds, monomer equivalent)

^{FAM}Aβ42/Aβ42 co-aggregation (0.1/10 µM) reactions in the absence and presence of SCL (10 µM). Lower panels represent magnifications of selected areas.

Fig. S3. The anti-Aβ antibody 352 preferentially detects β-sheet-rich Aβ42 aggregates in dot blot assays. (a) ThT binding assay. Short time incubation of fibrillar Aβ42 aggregates (25 µM) and Aβ42 monomers (25 µM) with ThT (25 µM). ThT binding assays indicate that fibrillar Aβ42 aggregates but not monomers are β-sheet-rich structures. **(b)** Analysis of preformed fibrillar aggregates and monomers with dot blot assays. The monoclonal antibody 352 detects fibrillar ThT-reactive Aβ42 aggregates but not monomers. **(c)** AFM analysis confirms that fibrillar Aβ42 aggregates (10 µM, monomer equivalent) are recognised by the 352 antibody.

Fig. S4. SCL treatment prevents the formation of SDS-stable ^{FAM}Aβ42/ Aβ42 co-aggregates. (a) Analysis of SCL-treated (10 µM) and untreated ^{FAM}Aβ42/Aβ42 co-aggregation reactions by denaturing FRAs. Compound treatment prevents the time-dependent formation of SDS-instable ^{FAM}Aβ42/Aβ42 co-aggregates. **(b)** Quantification of SDS-stable aggregates retained on filter membranes from **a**. Values are means ± SD, n = 3. Asterisks indicate significant differences as determined by the student t-test: * ≤ 0.05, ** ≤ 0.01, *** ≤ 0.001.

Fig. S5. SCL treatment decreases ThT binding to spontaneously formed Aβ42 aggregates. Aβ42 monomers (25 µM) were incubated with different concentrations of SCL (1, 10, 30 µM) for 15 h to obtain higher molecular weight aggregates. Then, ThT (25 µM) was added to reactions and fluorescence emission at 485 nm was measured. Values are means

± SD, n = 3. Asterisks indicate significant differences as determined by the student t-test: * ≤ 0.05, ** ≤ 0.01, *** ≤ 0.001.

Fig. S6. SCL-treatment decreases the seeding activity of spontaneously formed Aβ42 assemblies. (a) Schematic representation of Aβ42 seeding experiments with FP assays. First, Aβ42 monomers (10 μM) were incubated for 18 h in the presence and absence SCL (10 μM) to produce preformed aggregates (pAgg and pAgg+SCL). Second, the generated structures were added to ^{FAM}Aβ42/Aβ42 co-aggregation assays to monitor their seeding activity. **(b)** Effects of preformed Aβ42 seeds (250 nM, pAgg and pAgg+SCL) on spontaneous Aβ42 aggregation (25 μM) in ThT (25 μM) dye-binding assays. In control experiments, equivalent SCL concentrations (250 nM) without preformed Aβ42 aggregates were added to the ThT-based Aβ42 aggregation reactions. Values are means ± SD, n = 4 **(b)**.

Fig. S7. Inhibitory activity of SCL on spontaneous Aβ42 aggregation monitored by NMR. (a) 2D ^{1}H,^{15}N-HSCQ correlation spectrum of an Aβ42 (50 μM, ^{15}N uniform label) aggregation reaction after 0 and 24 h at 300K. **(b)** ^{1}H,^{15}N-HSCQ correlation spectrum of an Aβ42 (50 μM, ^{15}N uniform label) aggregation reaction with an equimolar concentration of SCL after 0 and 24 h at 300K.

Fig. S8. Investigating the interaction between Aβ42 peptides and SCL with 1D NMR WaterLOGSY experiments. (a) Reference 1H-1D spectrum of 500 μM sclerotiorin (SCL) in buffer with DMSO. **(b)** WaterLOGSY spectrum of 500 μM sclerotiorin in buffer with DMSO, all signals have the opposite (negative) sign compared to the H_2O signal, indicating that the compound is not aggregated in aqueous solution. **(c)** NMR WaterLOGSY spectrum

of 50 μM SCL in buffer with 50 μM Aβ42. No SCL signals are detectable, while signals of Aβ42 are visible, indicating that soluble Aβ42 peptides are present in solution but SCL binding cannot be detected under these experimental conditions. **(d)** WaterLOGSY spectrum of 500 μM SCL in the presence of 50 μM Aβ42 peptides. Signals for SCL are detectable, while signals for Aβ42 peptides are vanished, indicating that the compound binds to Aβ42 aggregates, which cannot be detected by solution WaterLOGSY NMR.

Fig. S9. SCL treatment decreases the formation of TAMRA-labeled fibrillar Aβ42 aggregates in cell-free assays. Compound treated and untreated samples were analysed by AFM after 18h of incubation at 37°C. Lower row, magnifications from upper row.

Supplemental Figures

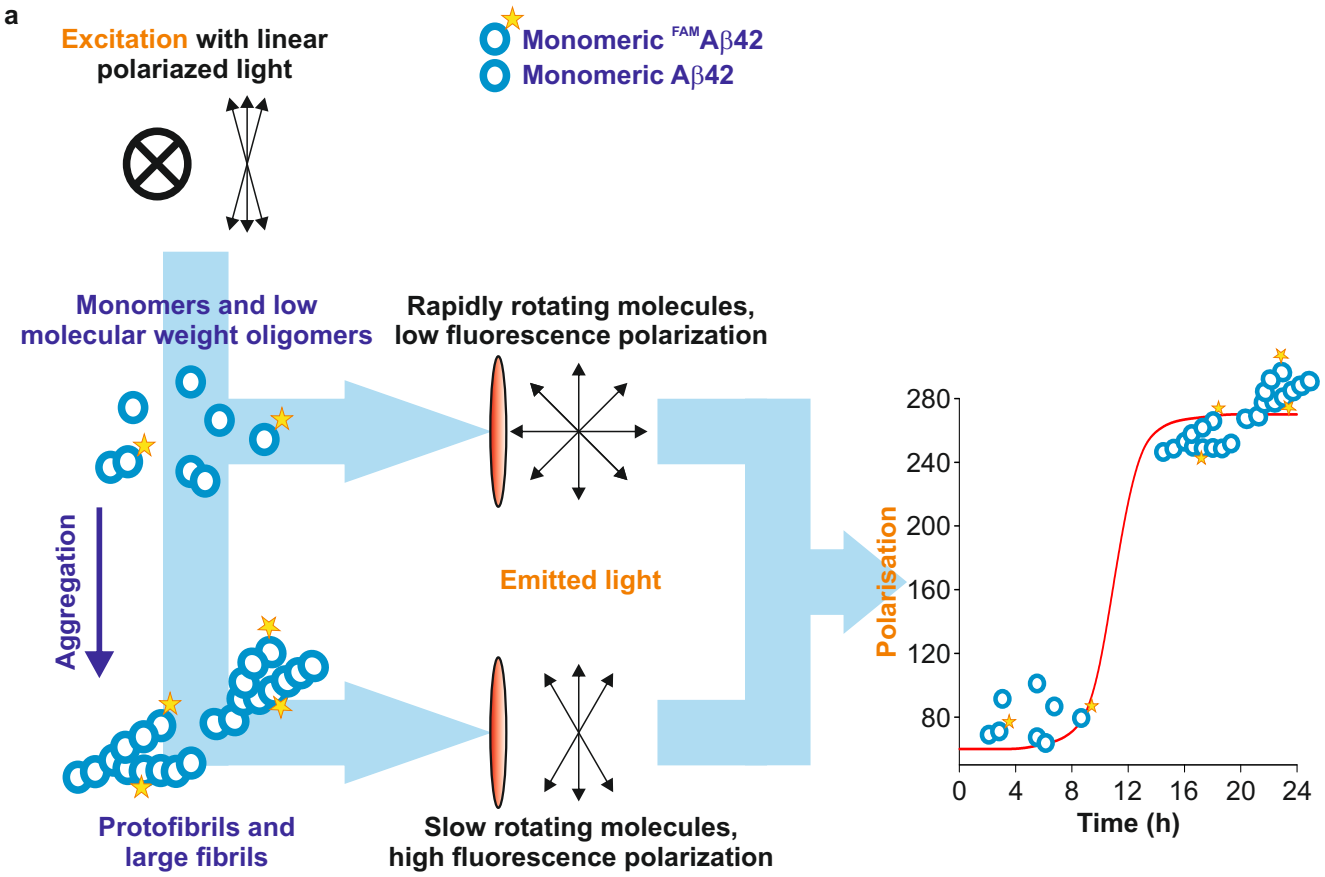

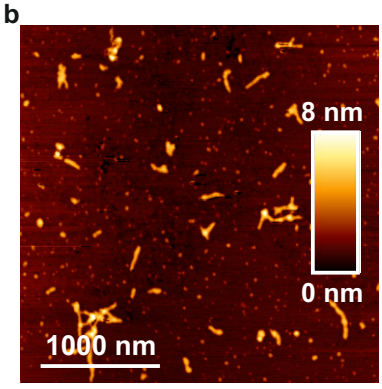

Fig. S1

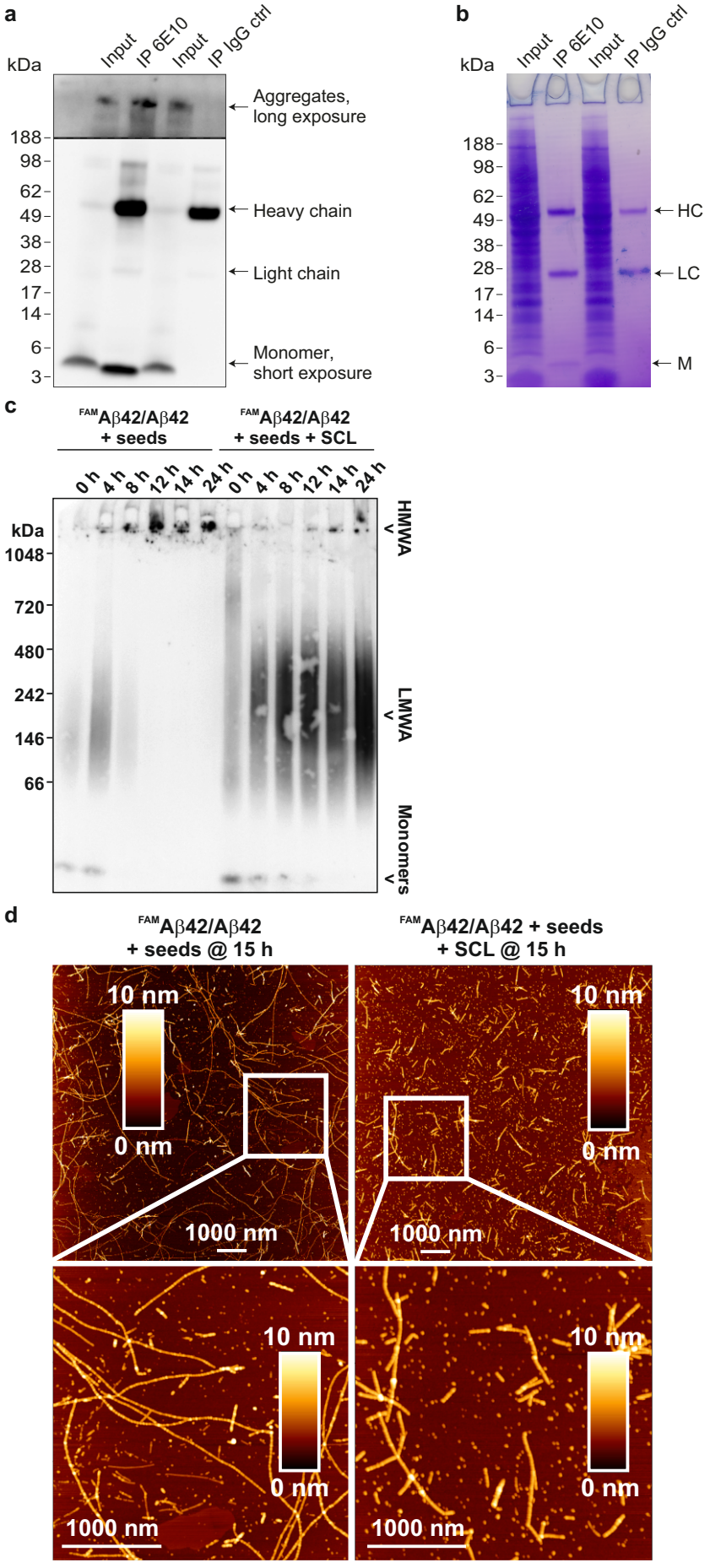
a
kDa
Input
IP 6E10
Input
IP IgG ctrl
188
98
62
49
38
28
17
14
6
3
Aggregates, long exposure
Heavy chain
Light chain
Monomer, short exposure
b
kDa
Input
IP 6E10
Input
IP IgG ctrl
188
98
62
49
38
28
17
14
6
3
HC
LC
M
c
FAMAβ42/Aβ42 + seeds
FAMAβ42/Aβ42 + seeds + SCL
0 h
4 h
8 h
12 h
14 h
24 h
kDa
1048
720
480
242
146
66
HMWA
LMWA
Monomers
d
FAMAβ42/Aβ42 + seeds @ 15 h
FAMAβ42/Aβ42 + seeds + SCL @ 15 h
10 nm
0 nm
1000 nm

Fig. S2

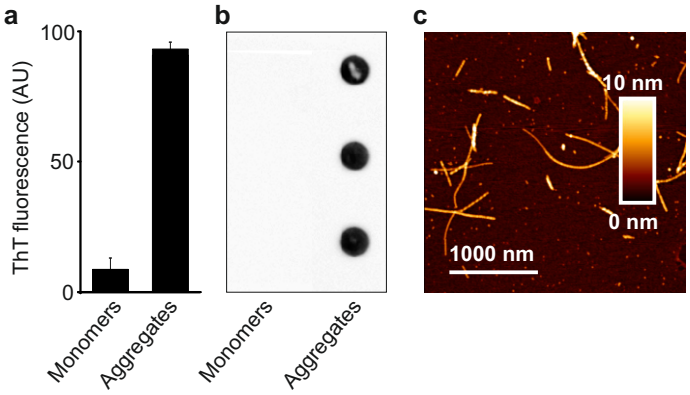
a
b
c
100
50
0
ThT fluorescence (AU)
Monomers
Aggregates
Monomers
Aggregates
10 nm
0 nm
1000 nm

Fig. S3

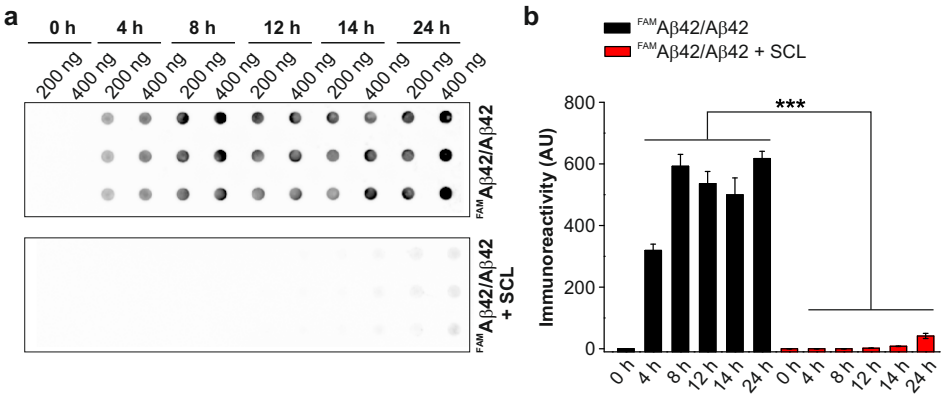
a
0 h
4 h
8 h
12 h
14 h
24 h
200 ng
400 ng
FAM Aβ42/Aβ42
FAM Aβ42/Aβ42 + SCL
b
FAM Aβ42/Aβ42
FAM Aβ42/Aβ42 + SCL
Immunoreactivity (AU)
800
600
400
200
0
***
0 h
4 h
8 h
12 h
14 h
24 h

Fig. S4

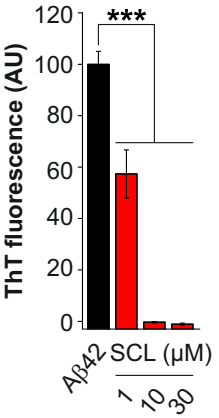

Fig. S5

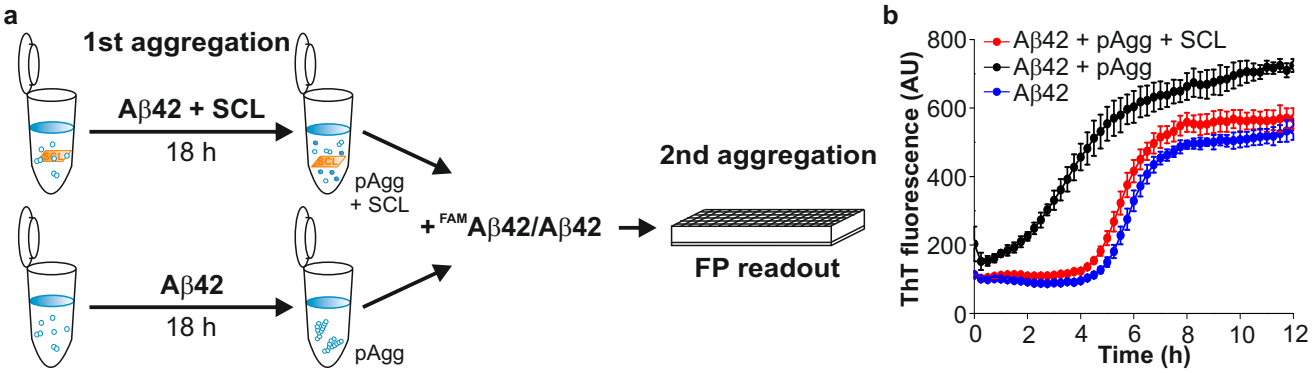
a
1st aggregation
Aβ42 + SCL
18 h
pAgg
+ SCL
Aβ42
18 h
pAgg
+ FAM Aβ42/Aβ42
2nd aggregation
FP readout
b
Aβ42 + pAgg + SCL
Aβ42 + pAgg
Aβ42
ThT fluorescence (AU)
800
600
400
200
0
0
2
4
6
8
10
12
Time (h)

Fig. S6

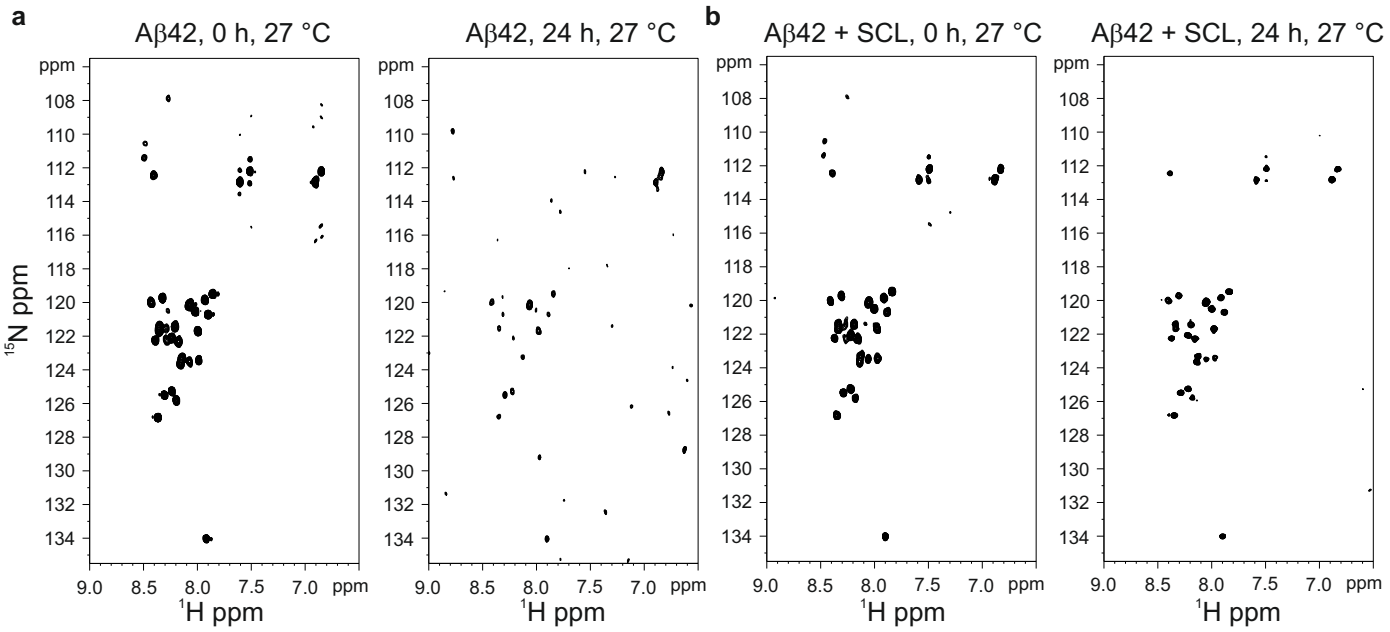
a
Aβ42, 0 h, 27 °C
Aβ42, 24 h, 27 °C
b
Aβ42 + SCL, 0 h, 27 °C
Aβ42 + SCL, 24 h, 27 °C
ppm
108
110
112
114
116
118
120
122
124
126
128
130
132
134
15N ppm
9.0
8.5
8.0
7.5
7.0
ppm
1H ppm

Fig. S7

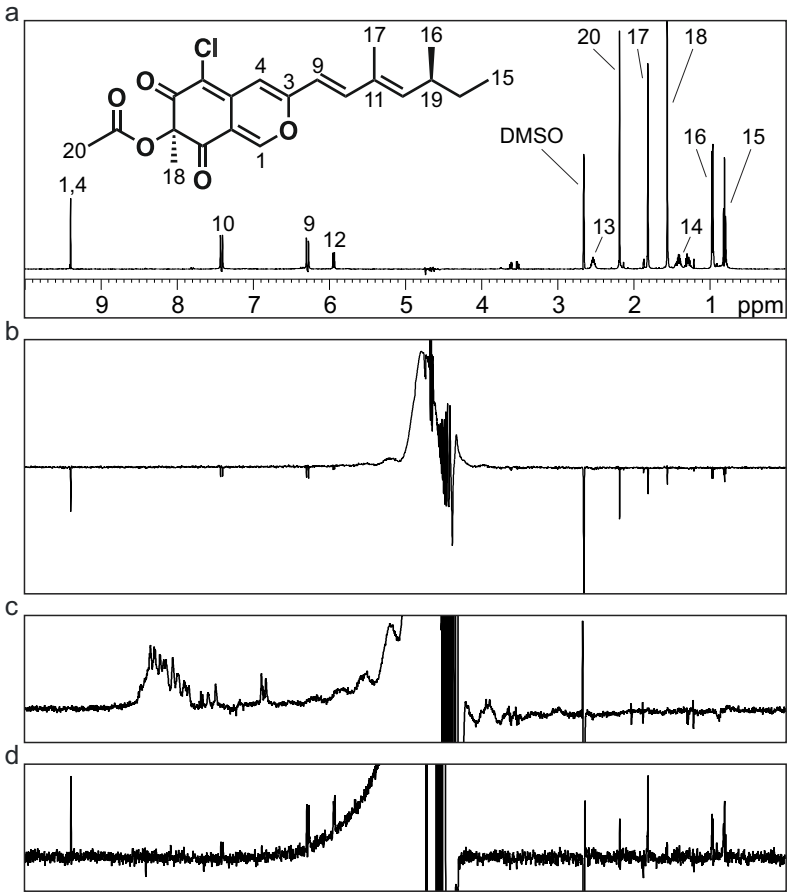
a
Cl
O
O
O
O
O
O
20
18
1
4
3
9
11
17
16
19
15
1,4
10
9
12
DMSO
13
20
17
18
16
14
15
9
8
7
6
5
4
3
2
1
ppm
b
c
d

Fig. S8

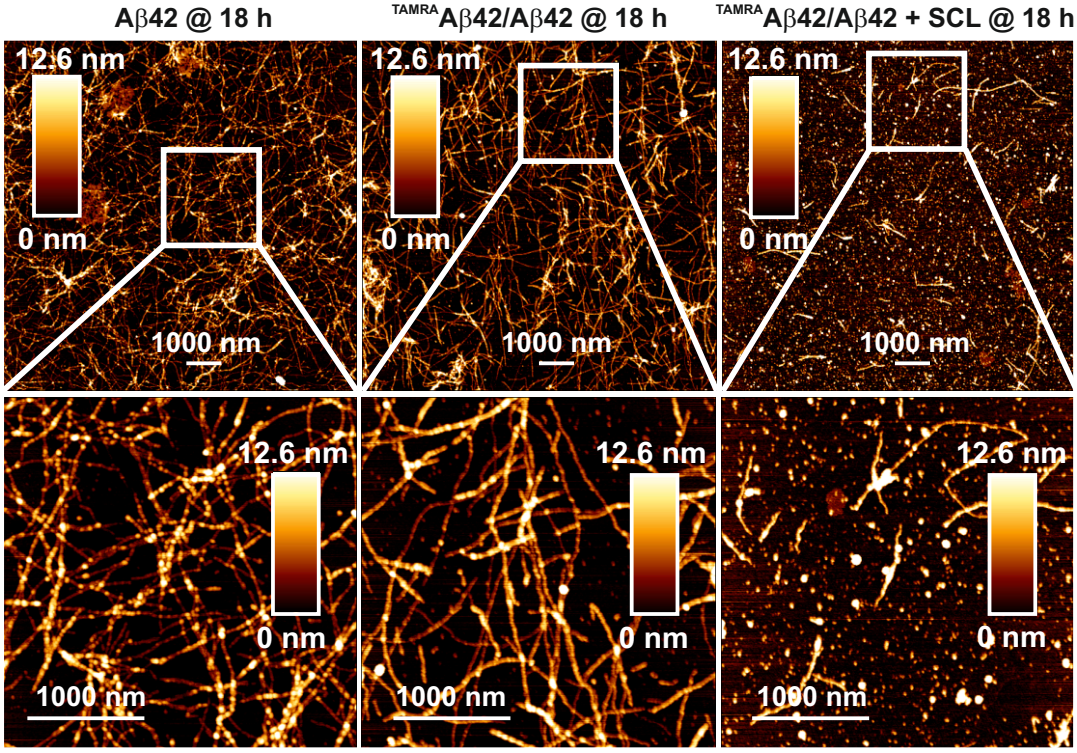
Aβ42 @ 18 h
TAMRAAβ42/Aβ42 @ 18 h
TAMRAAβ42/Aβ42 + SCL @ 18 h
12.6 nm
0 nm
1000 nm

Fig. S9